

The Pyrolysis of Isoxazole Revisited: A New Primary Product and the Pivotal Role of the Vinylnitrene. A Low-Temperature Matrix Isolation and Computational Study

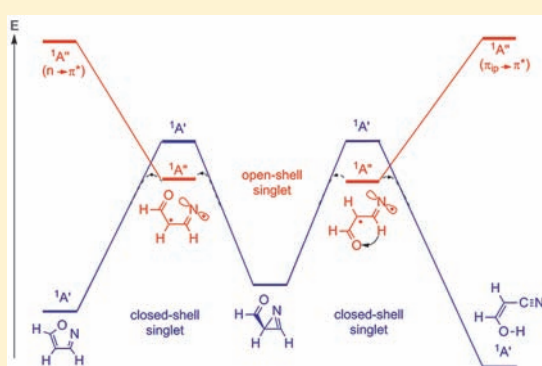
Cláudio M. Nunes,[†] Igor Reva,^{*,†} Teresa M. V. D. Pinho e Melo,[†] Rui Fausto,[†] Tomáš Šolomek,^{§,L} and Thomas Bally^{*,§}

[†]Department of Chemistry, University of Coimbra, P-3004-535 Coimbra, Portugal

[§]Department of Chemistry, University of Fribourg, CH-1700 Fribourg, Switzerland

 Supporting Information

ABSTRACT: This paper describes the pyrolysis of parent isoxazole and of its 5-methyl and 3,5-dimethyl derivatives by the high-pressure pulsed pyrolysis method, where activation of the precursor molecule occurs predominantly by collisions with the host gas (Ar in our case), rather than with the walls of the pyrolysis tube, where catalyzed processes may occur. The products were trapped at 15 K in Ar matrices and were characterized by vibrational spectroscopy. Thereby, hitherto unobserved primary products of pyrolysis of isoxazole and of its 5-methyl derivative, 3-hydroxypropenenitrile or 3-hydroxybutenenitrile, respectively, were observed. *E*–*Z* photoisomerization could be induced in the above hydroxynitriles. On pyrolysis of isoxazole, ketenimine and CO were observed as decomposition products, but this process did not occur when the 5-methyl derivative was pyrolyzed. Instead, the corresponding ketonitrile was formed. In the case of 3,5-dimethylisoxazole, 2-acetyl-3-methyl-2*H*-azirine was detected at moderate pyrolysis temperatures, whereas at higher temperatures, 2,5-dimethyloxazole was the only observed rearrangement product (next to products of dissociation). These findings are rationalized on the basis of quantum chemical calculations. Thereby it becomes evident that carbonyl-vinylnitrenes play a pivotal role in the observed rearrangements, a role that had not been recognized in previous theoretical studies because it had been assumed that vinylnitrenes are closed-shell singlet species, whereas they are in fact open-shell singlet biradicaloids. Thus, the primary processes had to be modeled by the multiconfigurational CASSCF method, followed by single-point MR-CISD calculations. The picture that emerges from these calculations is in excellent accord with the experimental findings; that is, they explain why some possible products are observed while others are not.



1. INTRODUCTION

Isoxazoles (compounds **1** in Scheme 1) are heterocyclic compounds that have a number of applications in areas as diverse as pharmaceuticals, agrochemistry, molecular electronics, corrosion inhibition, and liquid crystals.^{1,2} They are found in natural sources; well-known examples are ibotenic acid and muscimol, powerful psychoactive and neurotoxic compounds isolated from fungi.² Much of the chemistry of isoxazoles is initiated by the cleavage of its weak N–O bond, which has been shown, for example, to occur during the biotransformation of several isoxazole-containing drugs.^{3–5} Isoxazoles can also be functionalized, which make them important building blocks in organic synthesis.^{1,2,6}

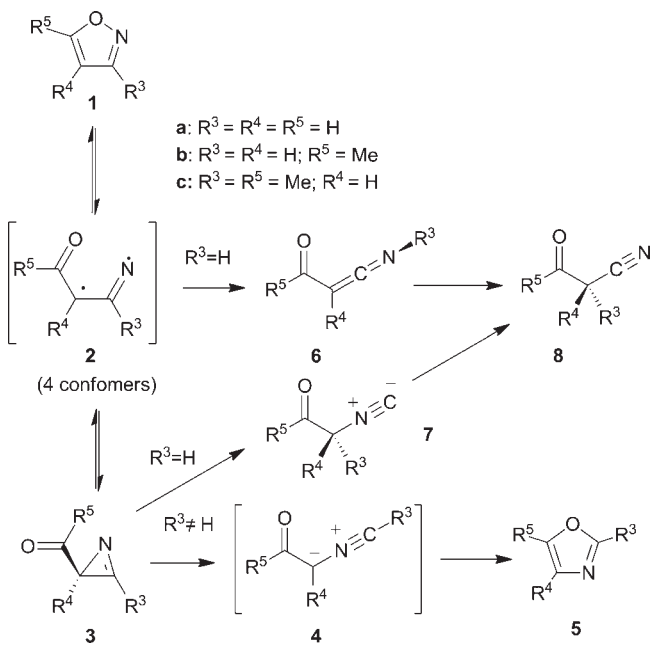
The thermolysis of isoxazoles has been the subject of several studies.^{1,2,6} Under conditions of flash vacuum pyrolysis (FVP), most isoxazoles **1** were found to isomerize into the corresponding 2*H*-azirines **3**, oxazoles **5**, or 3-oxopropanenitriles **8**.^{7–14} Based on these results and on kinetic and theoretical studies, the

general mechanism shown in Scheme 1 was proposed.^{14,15} First, isoxazoles **1** isomerize to 2*H*-azirines **3** through N–O bond cleavage (involving the putative vinylnitrene intermediate **2** or via a concerted [1,3]-sigmatropic shift). The 2*H*-azirines **3** could subsequently undergo C–C bond scission to yield nitrile ylides **4**, followed by cyclization to the corresponding oxazoles **5**. If R³ = H, the C–C scission may be accompanied by a hydrogen shift to yield isocyanides **7**. [1,2]-H-shift in **1** or **2** may lead to ketenimines **6**. Both **6** and **7** can in turn yield nitriles **8**.

The final products of the gas-phase thermolysis of isoxazoles **1** depend on the nature of the substituents R³ and R⁵. The reported results on the FVP of 5-methylisoxazole,⁹ 5-amino-4-methylisoxazole,⁹ and 4-acetyl-5-methylisoxazole¹¹ indicate that when R³ = H the preferential pathway is H migration and the formation of nitriles **8** whereas if R³ = Me or R³ = NH₂ oxazoles are formed instead.¹⁴

Received: August 15, 2011

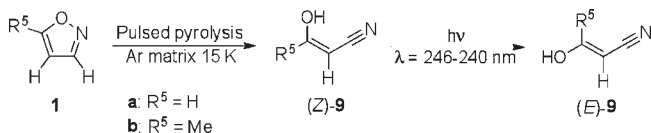
Published: September 28, 2011

Scheme 1. Proposed Mechanism of Isoxazole Pyrolysis^{14,15}

On the other hand, only decomposition products were formed in shock tube thermal reactor experiments of parent isoxazole **1a** and 5-methylisoxazole **1b**.^{16,17} Acetonitrile and carbon dioxide, followed by hydrogen cyanide and ketene, were found in the former case, while propionitrile and carbon monoxide, followed by ethane, methane, acetonitrile, and hydrogen cyanide, were identified in the latter. Based on these findings, it was proposed that the decay mechanism of isoxazole **1a** and 5-methylisoxazole **1b** involved only unimolecular decomposition processes.^{16–18} However, subsequent theoretical studies suggested that **1a** and **1b** should isomerize before decomposition,^{15,19} in line with the above-mentioned FVP results.

The most recent *ab initio* calculations¹⁵ predict that the thermolysis of **1** should involve the initial formation of the corresponding *2H*-azirines **3** in a concerted process, bypassing the vinylnitrenes **2**, which were found not to be potential energy minima. These calculations predicted also that the rearrangement of azirines **3** to isonitriles **7**, which isomerize easily to nitriles **8**, has a lower activation energy than their isomerization to oxazoles **5**, either by a concerted mechanism or by a stepwise process involving the nitrile ylides **4** as metastable intermediates.

Despite the above-described attempts to elucidate the mechanism of the thermolysis of isoxazoles by experimental and theoretical means, it is still far from being well understood. In the present work, we report the results of a study of the thermolysis of isoxazole **1a**, 5-methylisoxazole **1b**, and 3,5-dimethylisoxazole **1c** in an argon atmosphere using the technique of pulsed pyrolysis and isolation of the products in a matrix at 10–20 K, conditions under which bimolecular reactions are largely inhibited, and where the products can be characterized by well-resolved IR spectra. Thus, we were able to show that **1a** and **1b** engage in a hitherto unknown rearrangement leading to (*Z*)-3-hydroxypropenenitriles **9**, which could subsequently be photoisomerized by UV-irradiation to their *E* isomers (Scheme 2). In contrast, **1c** formed the previously identified products, azirine **3c** and oxazole **5c**.⁸

Scheme 2. Pulsed Pyrolysis of Isoxazoles **1a** and **1b** Generates (*Z*)-3-Hydroxypropenenitriles **9a** and **9b** That Photoisomerize to Their *E* Counterparts

Concurrently, we engaged in quantum chemical calculations to simulate and assign the observed IR spectra and to model the potential surfaces on which the observed rearrangements take place. We paid particular attention to the possible involvement of the elusive yet pivotal vinylnitrene **2**, which is known to have a triplet ground state and whose lowest singlet state is of *open-shell* nature.^{20–22} These features, which have not been considered in previous theoretical studies of isoxazole rearrangements, require that multiconfigurational methods be used in modeling the potential surfaces. We highlight the pivotal role of the vinylnitrene intermediate **2**, which resides on a very flat part of the potential surface but by which the reactions leading to many of the identified products, including the newly found hydroxypropenenitriles **9**, proceed. The reason this has been ignored in previous theoretical studies is that the vinylnitrene was invariably assumed to be in its (excited) closed-shell singlet state, instead of allowing it to relax to its lower-lying open-shell singlet state.

2. RESULTS AND DISCUSSION

2.1. IR Spectra of Matrix-Isolated Isoxazole and 5-Methylisoxazole. Figure 1 shows the experimental and the calculated IR spectra obtained after room-temperature pulsed deposition of **1a** and **1b**. Comparison of the IR spectrum of **1a** in an argon matrix with that obtained in gas phase^{23–25} shows excellent agreement (the maximum deviation in the region between 500 and 1700 cm^{-1} is 3 cm^{-1} ; see Table S1, Supporting Information, which shows also the assignment of all observed bands to calculated normal modes). This indicates the absence of significant interaction between **1a** and the argon host gas and suggests that **1a** is isolated as a monomer in the matrix. The similar high quality of the spectra of **1b** and **1c** suggests that the same applies for these derivatives.

2.2. Pulsed Pyrolysis Experiments. **2.2.1. Isoxazole 1a.** On pulsed pyrolysis of a gas phase mixture of **1a** and Ar (~1:1000), new IR bands began to appear when the SiC tube was heated to ca. 600 °C (for details see section 3.1). As the temperature increased to 800 °C, the bands of **1a** diminish in intensity, while those of products increase. We were able to identify the presence of carbon monoxide due to its characteristic band at 2138 cm^{-1} ;²⁶ two other dominant products, labeled temporarily as **A** and **B**, were apparently formed (Figure 2).

The most intense of the product bands appears at 2037/2039 cm^{-1} . Because it is known that ketenimines $R_2C=C=NR$ generally absorb strongly in the 2000–2100 cm^{-1} region,^{27–29} we attribute this band, which is split into two components by a site effect, to an $N=C=C$ antisymmetric stretching mode.³⁰ The formylketenimine **6a** (see Scheme 1) was apparently not formed, because no band due to the $C=O$ stretching mode of its aldehyde moiety was observed.³¹ However, all bands labeled **A** in Figure 2 are in perfect accord with the reported infrared

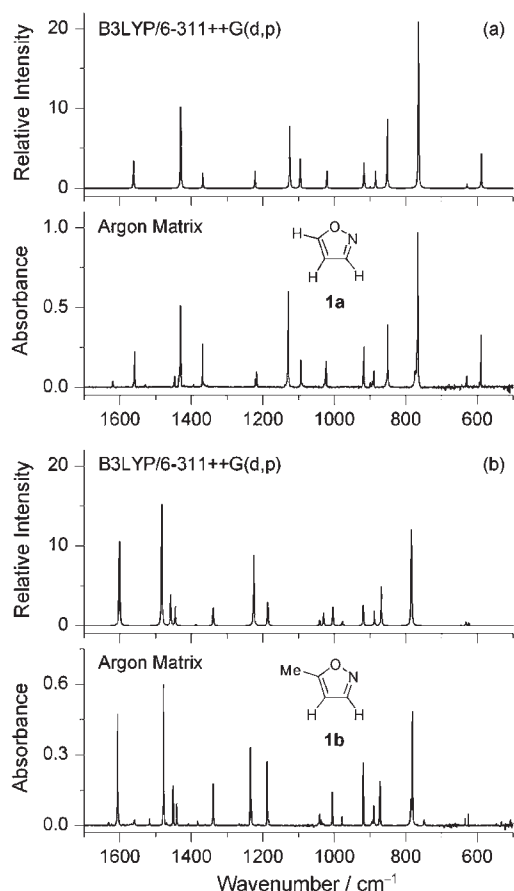


Figure 1. (a) Experimental FTIR spectra of isoxazoles **1a** (a) and **1b** (b) isolated in argon matrices at 15 K and the respective IR spectra calculated by the B3LYP method (details, see section 3.2).

spectrum^{32–34} of the parent ketenimine ($\text{H}_2\text{C}=\text{C}=\text{NH}$, **10**; Table 1). The presence of CO as a byproduct in the formation of **10** in the pyrolysis of **1a** is expected and is readily established (*vide supra*).

The IR spectrum of the other main product, **B**, in Figure 2 differs from those measured or calculated for any of the expected and previously observed products of the thermolysis of **1a**, that is, 2*H*-azirine-2-carbaldehyde **3a**, oxazole **5a**, 2-isocyanoacetaldehyde **7a**, or 3-oxopropanenitrile **8a** (See Scheme 1). There are two very informative bands in the IR spectrum of **B**: one at 2222 cm^{-1} , in the region of $\text{C}\equiv\text{N}$ stretching vibrations of nitriles,³⁵ and another at $3544/3539\text{ cm}^{-1}$, that is, in a region of OH stretching vibrations.

These findings led us to investigate the possible formation of 3-hydroxypropenenitrile **9a**, a molecule that has hitherto never been considered or observed in thermolyses of **1a**. Compound **9a** could conceivably be formed by enolization of **8a**, by a [1,4]-H-shift from **2a** or **3a**, or by a [1,5]-H-shift from **6a**. Compound **9a** exists in the four conformations shown in Scheme 3, which were all found to represent potential energy minima on the B3LYP/6-311++G(d,p) potential surface.

We found that the calculated infrared spectrum of the most stable *syn*-(*Z*) conformer of **9a** is the only one that compares well with that of product **B**. Figure 3 shows the excellent agreement between experiment and calculation for a 1:2 mixture of *syn*-(*Z*)-**9a** and ketenimine **10** + CO.

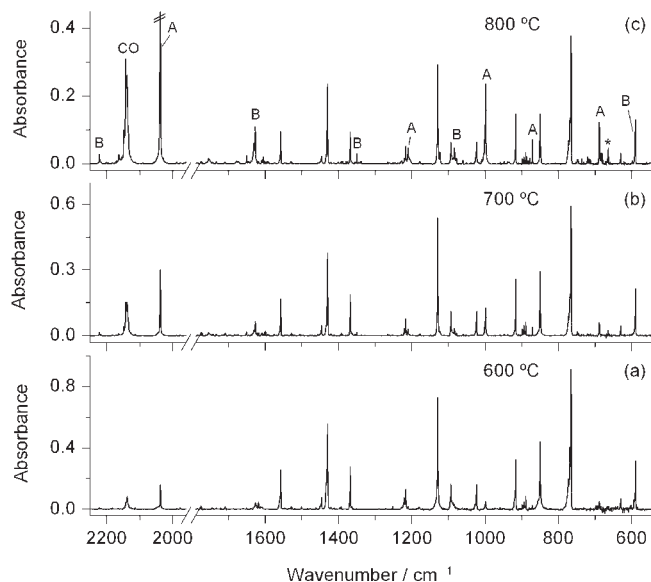
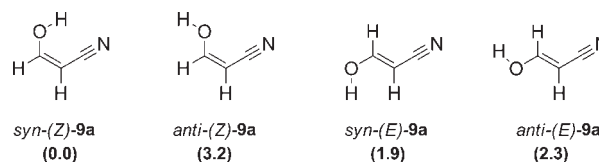


Figure 2. Experimental IR spectra of products of pulse pyrolysis of isoxazole **1a** trapped in argon matrices at 15 K. The temperature of the SiC tube was at (a) 600, (b) 700, and (c) 800 °C. The new major bands in spectrum (c) are assigned to two species labeled A and B. The band marked with an asterisk is due to an impurity from the pyrolyzer system.

Scheme 3. Conformers of 3-Hydroxypropenenitrile **9a**^a



^a Values in parentheses represent the relative B3LYP/6-311++G(d,p) calculated energies in kcal/mol (including ZPE corrections).

When the matrix obtained on 800 °C pyrolysis of isoxazole **1a** was subjected to 240 nm laser irradiation (until a photostationary state was reached), new IR peaks, shown in Figure 4a, appeared with concomitant intensity decrease of those of *syn*-(*Z*)-**9a** (note that the peaks of **1a**, for example, at 1430 cm^{-1} , did not change during that photolysis). The calculated spectra of the four conformers of **9a** revealed that *syn*-(*Z*)-**9a** was photoisomerized into a mixture of *syn*-(*E*)-**9a** and *anti*-(*E*)-**9a**, as evidenced in Figure 4b. Detailed results from the calculations and IR assignments are presented in Tables S3 and S4 in the Supporting Information. The observed shifts of $\nu(\text{OH})$ to higher frequencies in the *E*-conformers of **9a** reflect the disruption of the intramolecular interaction involving the (O)–H and the in-plane $\text{C}\equiv\text{N}$ π -bond, which is present only in the most stable *syn*-(*Z*) conformer (the OH bond length in that conformer is also the longest of all four). The absence of this hydrogen bonding interaction may also be the reason for the lower stability of the other conformers.

Our results indicate that *syn*-(*Z*)-**9a** is, within the detection limits, the only conformer obtained in pulsed pyrolysis of **1a**, suggesting that **9a** is formed in a stereospecific fashion. Examples of thermal processes that yield a specific conformer have been reported for other systems.^{36–40} It is difficult to assess the temperature of samples after they exit the pulsed pyrolysis tube, except that it must be lower than the temperature at which the

Table 1. Comparison of Our Experimental with Previously Reported IR Spectra of Ketenimine 10

experimental spectrum ^a this work	experimental spectra ^b previously reported		sym	assignment ^c
3298 (w)			A'	$\nu(\text{NH})$
2039/2037 (vs)	2040 (vs)	2033.9 (100)	A'	$\nu(\text{N}=\text{C}=\text{C})_{\text{as}}$
1124 (w)	1124 (w)		A'	$\nu(\text{N}=\text{C}=\text{C})_{\text{s}} + \delta\text{CH}_2(\text{scis})$
999 (s)	1000 (s)	992.7 (30)	A'	$\delta(\text{CNH})$
871 (m)	872 (m)	882.8 (24)	A''	$\tau(\text{NH})$
689 (m)	690 (m)	689.3 (13)	A'	$\gamma(\text{H}_2\text{CC})$

^a Argon matrix at 15 K. Band positions in cm^{-1} ; experimental intensities in parentheses are presented in qualitative terms: vs = very strong, s = strong, m = medium, w = weak. ^b Refs 32–34. ^c Symbol: ν , bond stretching; δ , bending; γ , out-of-plane bending; τ , torsion; as, antisymmetric; s, symmetric; scis, scissoring.

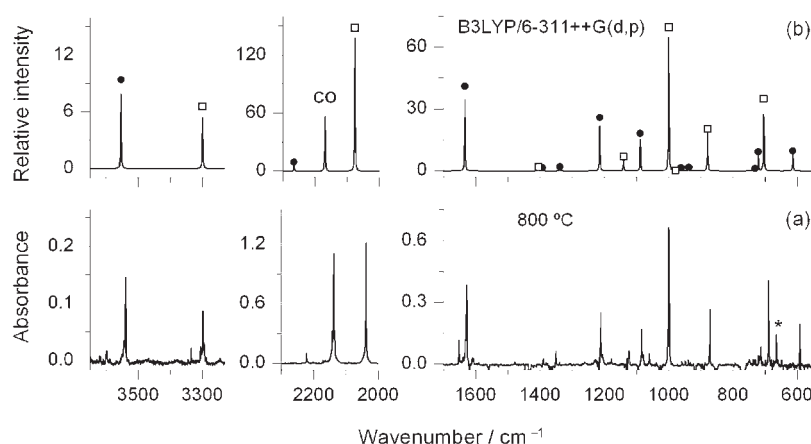


Figure 3. (a) IR spectrum obtained on pyrolysis of isoxazole **1a** at 800 °C and the products isolated in an argon matrix at 15 K, where the bands of the remaining precursor were subtracted. (b) IR spectrum of *syn*-(*Z*)-**9a** (●), and **10** (□) (ratio 0.5:1), along with CO, simulated on the basis of B3LYP calculations (details see section 3.2). The band marked with asterisk is due to an impurity from the pyrolyzer system.

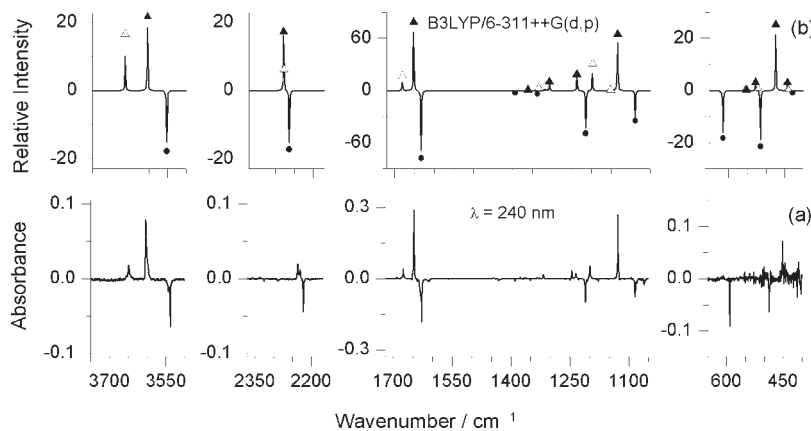


Figure 4. (a) Changes in the experimental IR spectrum of **1a** subjected to pyrolysis at 800 °C, with the products isolated in an argon matrix at 15 K, which occur upon 15 min of irradiation of this matrix with UV ($\lambda = 240 \text{ nm}$) light (growing bands point upward), monitoring the photoinduced conformational isomerization of *syn*-(*Z*)-**9a** (negative bands) into *syn*-(*E*)-**9a** and *anti*-(*E*)-**9a** (positive bands) in matrix-isolated **9a** at 15 K. (b) Simulated difference IR spectrum obtained as [20% *anti*-(*E*)-**9a** (Δ) + 80% *syn*-(*E*)-**9a** (\blacktriangle)] minus [*syn*-(*Z*)-**9a** (\bullet)], based on B3LYP calculations (details, see section 3.2).

tube is held (because thermal equilibrium is not established in a pulsed flow system). According to thermochemical calculations,⁴¹ the other three conformers should be within 2–3 kcal/mol of *syn*-(*Z*)-**9a** on a free energy scale and should therefore be present in proportions of 6–9% at 300 °C up to 14–18% at 700 °C, which should be detectable. If enough energy is available to

cleave the N–O bond in **1a**, this should also suffice to induce rotation around the double bond in **9a**,⁴² let alone the C–O bond, so the other conformers should be kinetically accessible. Nevertheless, we found other reaction channels with lower energy than that required to rotate the double bond in *syn*-(*Z*)-**9a** (see the section on mechanistic molecular modeling).

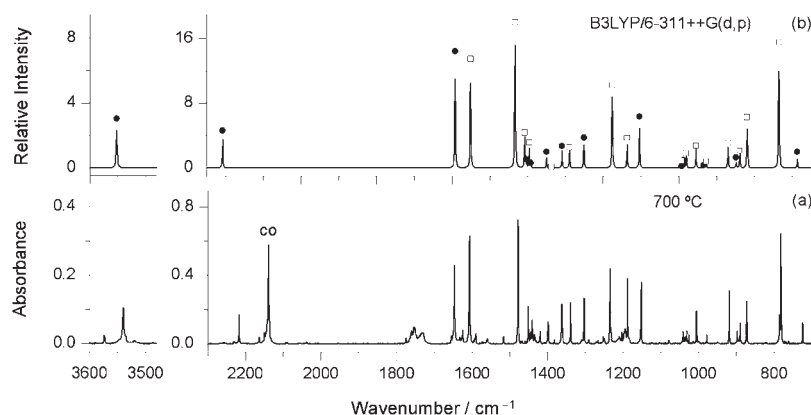


Figure 5. (a) Experimental IR spectra of products of pulse pyrolysis (700 °C) of 5-methylisoxazole **1b** trapped in an argon matrix at 15 K; (b) simulated IR spectrum of *syn*-(*Z*)-**9b** (●) and **1b** (□) (assuming the ratio of 1:9) on the basis of B3LYP calculations (details see section 3.2).

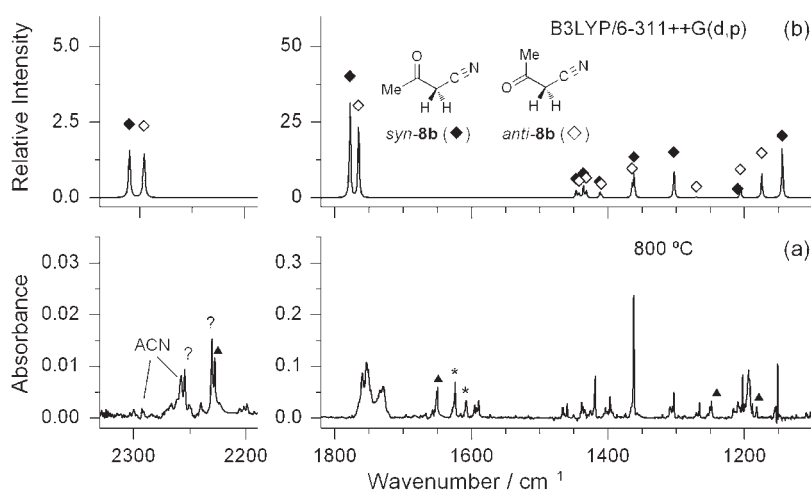
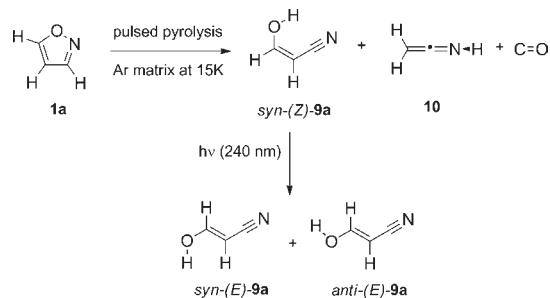


Figure 6. (a) Experimental IR spectrum of the products of pulse pyrolysis of 5-methylisoxazole **1b** (when the temperature of the SiC tube is kept at 800 °C), trapped in an argon matrix at 15 K. The absorptions due to the reagent **1b** and *syn*-(*Z*)-**9b** were eliminated by subtraction of the scaled spectra of nonpyrolyzed **1b** and *syn*-(*Z*)-**9b** (see Figure S2 in the Supporting Information). Bands labeled with (▲) correspond to *syn*-(*E*)-**9b**; those labeled ACN correspond to acetonitrile. The peaks labeled with a question mark are tentatively assigned to the C≡N stretching vibrations of *syn*- and *anti*-**8b**. (b) Simulated IR spectrum of *syn*-**8b** (◆) and *anti*-**8b** (◇) (ratio 65%/35%, adjusted to experiment), based on B3LYP calculations (details see section 3.2).

Scheme 4. Summary of Observations from the Pulsed Pyrolysis of Isoxazole **1a**



In addition, “conformational cooling” occurs on supersonic expansion of the jet exiting the 1 mm ID pyrolysis tube, which might also lead to the depopulation of less stable conformers.^{43–46}

2.2.2. 5-Methylisoxazole 1b. Similar experiments as those described for **1a** were carried out with 5-methylisoxazole **1b**.

As an example, Figure 5a shows the spectrum obtained on pulsed pyrolysis of **1b** at 700 °C. Most of the bands in that spectrum belong to nonreacted **1b** or can be readily assigned to *syn*-(*Z*)-**9b**, as shown in Figure 5b. The same photoisomerization as found for **9a** can also be observed for the methyl derivative **9b** (see Figure S1 and Table S4, Supporting Information) further confirming the assignment.

The spectrum in which both the peaks of the precursor **1b** and of **9b** are subtracted is depicted in Figure 6a (details of the procedure are documented in the Supporting Information). The most conspicuous signal in this resultant spectrum is a double-humped band at 1750 cm⁻¹, which hints at the presence of two conformers of a ketone. The ketenimine **6b**, the isonitrile **7b**, or the nitrile **8b**, which might all be formed upon **1b** pyrolysis, all possess a keto group (cf. Scheme 1).

Ketenimine **6b** and isonitrile **7b** should have a strong band at around 2070 and 2170 cm⁻¹, respectively.⁴⁷ However, these spectral regions are almost empty in Figure 5a. In contrast, B3LYP calculations predict that the C≡N stretching vibration in

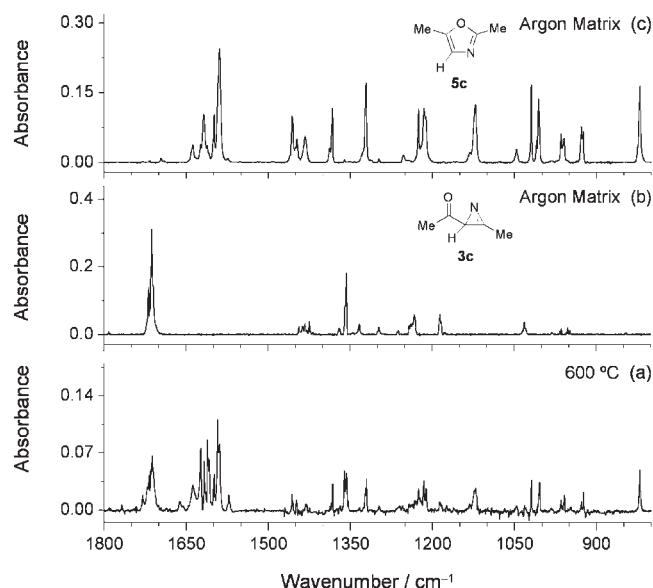


Figure 7. (a) Experimental IR spectrum of products of pulse pyrolysis of 3,5-dimethylisoxazole **1c** (when the temperature of the SiC tube is kept at 600 °C), trapped in an argon matrix at 15 K. The absorptions due to the reagent were eliminated (by subtraction of a scaled spectrum of the nonpyrolyzed **1c** isolated in an argon matrix, see Figure S3, Supporting Information, for the original spectra). (b,c) Experimental IR spectra of 2-acetyl-3-methyl-2H-azirine **3c** (b) and 2,5-dimethylisoxazole **5c** (c) isolated in argon matrices at 15 K in separate experiments.

nitrile **8b** gives rise to an IR band at 2306 cm^{-1} that is ~ 20 times less intense than that for the ketone C=O stretch. Indeed some weak new bands appear between 2200 and 2300 cm^{-1} , in concert with the C=O stretch at 1750 cm^{-1} , which are not incompatible with the predictions for **8b** (Figure 6). Figure 6b shows a simulated spectrum of the two conformers of **8b** (in a ratio that is in accord with the relative intensity of the two C=O bands). Therefore, ketonitrile **8b** appears to be the only viable candidate for the ketone that is formed on pyrolysis of **1b**.

No CO and ketenimine ($\text{H}_2\text{C}=\text{C}=\text{NMe}$, **10b**) are formed in the experiments with 5-methylisoxazole **1b**. Such a process would require a shift of the methyl group with concomitant C–C bond rupture to release CO. This reaction channel seems to be inaccessible when a substituent other than hydrogen is present in the 5-position of isoxazole. The fact that we observe instead ketonitrile **8b** in the pyrolysis of **1b** indicates that these fragments arise from nitrile **8b**.

2.2.3. 3,5-Dimethylisoxazole 1c. Figure 7 shows the results of the pyrolysis of 3,5-dimethylisoxazole **1c** at 600 °C, where we can distinguish, upon subtraction of the bands due to the remaining precursor, the IR bands of two products, namely, azirine **3c** (main bands around 1715 and 1360 cm^{-1}) and oxazole **5c** (most of the remaining bands) by comparison with their authentic matrix IR spectra, which are shown in traces b and c. At higher temperatures, the bands of **3c** disappear, while those of oxazole **5c** continue to grow. In addition, several new products begin to appear, whose definitive assignment will be presented in a separate publication.

The experimental findings for the pulsed pyrolysis of **1a** are summarized in Scheme 4. In the following section we will try to explain these findings by means of quantum chemical calculations.

2.3. Mechanistic Molecular Modeling. Undoubtedly, the first process in the thermolysis of isoxazoles is cleavage of the

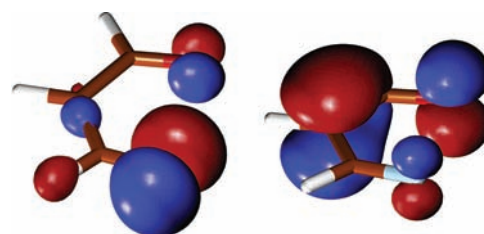


Figure 8. The two singly occupied MOs of formylvinylnitrene **2a** in its lowest singlet state from a CAS(8,7)SCF calculation (light blue is the N, red the O-atom).

weak N–O bond, which leads to the *syn*-(*Z*)-form of carbonylvinylnitrenes (structure **2** in Scheme 1). Conceptually these vinylnitrenes can decay to azirines **3** or, by different H-shifts, to carbonyl-ketenimines **6**, nitriles **8**, their enol forms **9**, or imino-ketenes **11**, as shown in Scheme 5 for the parent compound. We engaged in quantum chemical calculations to show why some of these products are apparently formed, while others are not, and how the secondary products that were observed in our study (ketenimine **10** + CO or oxazoles **5**) may arise.

In Scheme 5, it is implied that all stable products (**3**, **6**, **8**, **9**, and **11**) originate from different conformations of the vinylnitrene **2**. This must not necessarily be the case, as indicated by the dashed black lines which imply that, in the case of azirines **3**, C–N bond breaking and H-shifts may occur concomitantly, thus bypassing the vinylnitrenes **2**.

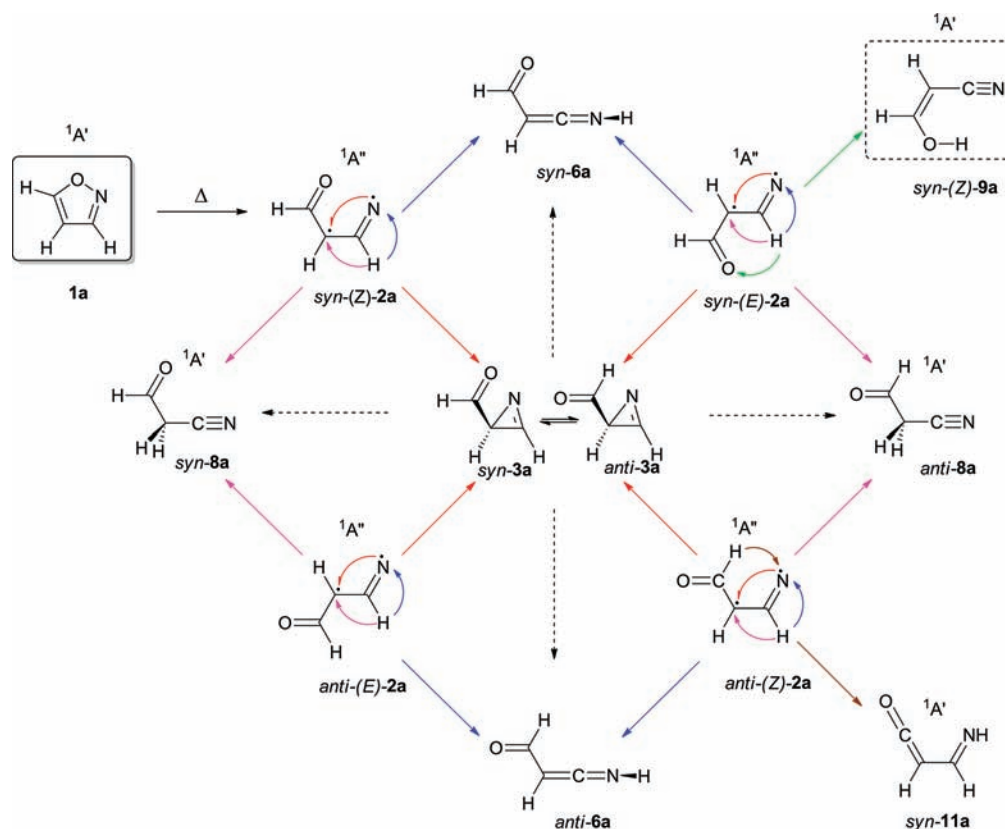
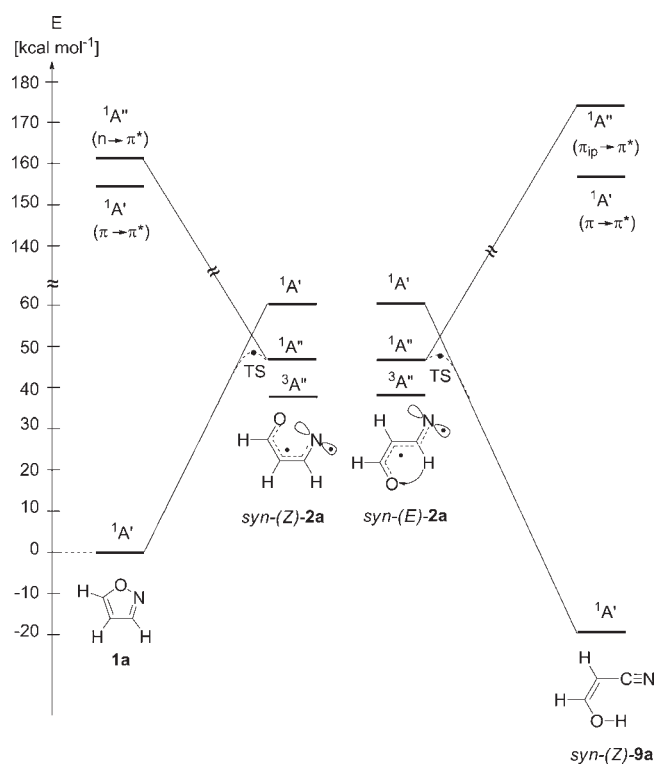
In fact, earlier computational studies of the thermolysis of isoxazoles^{15,19} have never found any evidence for the involvement of vinylnitrenes **2**. In contrast, it was noted that these species lie very high in energy and do not even represent stationary points on the potential energy surface. However, these studies failed to account for the fact that the lowest singlet states of vinylnitrenes are of *open-shell* (biradicaloid) nature, as was shown in the 1990s.^{20,21} Any calculations that force isoxazole to remain closed shell on the way to one or the other stable product will thus necessarily bypass the vinylnitrenes **2**, because the (excited) closed-shell singlet states of these species lie much higher in energy.

We thus decided to reinvestigate the rearrangements shown in Scheme 5 using the multiconfigurational CASSCF method, which allows for a smooth passage between closed- and open-shell singlet states, provided that the orbitals are averaged for the two states. Because dynamic correlation effects are known to be important in determining activation energies, we carried out single-point MR-CISD calculations at the CASSCF geometries (for details of these calculations see Methods).

Figure 8 shows the two MOs that are occupied by electrons of opposite spin in the lowest singlet state of formylvinylnitrene **2a**.

2.3.1. The Formation and Decay of Vinylnitrenes 2. In their seminal paper on the ring expansion of phenylnitrene,²¹ Karney and Borden pointed out, in a footnote, that on a CASSCF(4,4)/6-31G* potential surface, the lowest singlet state of parent vinylnitrene is a transition state for the interconversion of enantiotopic azirines. Our first step was thus to check whether formylvinylnitrenes **2a** are also transition states on a corresponding CASSCF surface. It turned out that three out of the four planar structures are actually (shallow) minima (the *anti*-(*Z*) geometry corresponds to a flat transition state), which decay, however, in almost (or completely) barrierless processes to one of the two conformations of azirine **3a**. Thus, the different planar

Scheme 5. Possible Decay Paths for Formylvinylidene 2a

Scheme 6. State Correlation Diagram for 1a, 2a, and 9a in C_s Symmetry^a

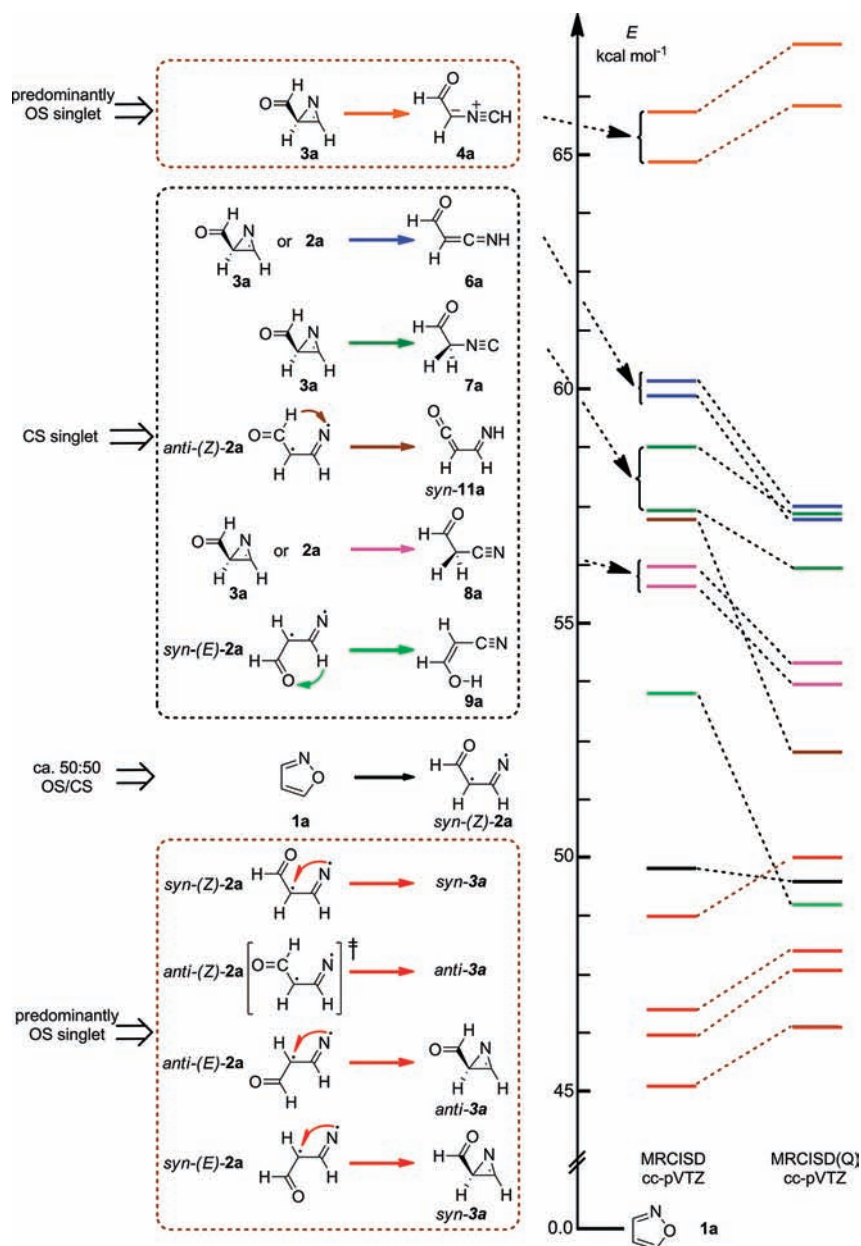
^a Semiquantitative, based on MR-CISD(Q) calculations.

forms of vinylidene 2a also serve as transition states for (or fleeting intermediates in) the interconversion of pairs of enantiomeric azirines 3. The different planar forms of 2a can in turn only interconvert via the azirines, to which the vinylidene collapses readily on twisting either of the central C–C bonds.

In a second step, we investigated the process of formation of 2a from isoxazole 1a. Thereby we noted that this reaction cannot take place in an adiabatic fashion in C_s symmetry because the ground state of isoxazole (as that of all planar closed-shell species in Scheme 5) is $1A'$ whereas the lowest singlet state of 2a has one electron in a σ - and one in a π -MO (see Figure 8) and has therefore $1A''$ symmetry. Thus, there will be a conical intersection in C_s symmetry, which must be circumvented by an out-of-plane distortion on the way from 1a to 2a and on the path from 2a to other planar products, such as 9a, shown as an example in Scheme 6.

Indeed we found that the transition state for the 1a \rightarrow 2a reaction is slightly nonplanar, and the wave function at this transition state is a mixture of closed- and open-shell configurations. At the MRCI level, the barrier is just under 50 kcal/mol (cf. Scheme 6), very close to the energy of *syn*-(Z)-2a, which is thus barely protected from decaying back to isoxazole 1a (note, however, that the other conformers of 2a lie slightly lower in energy).

Next we searched the transition states for the different hydrogen shift reactions that are indicated with differently colored arrows in Scheme 5. The lowest-lying of these transition states is for the stereospecific [1,3]-H-shift leading from the *syn*-(E) conformer of 2a (which is the most stable of the four

Scheme 7. MRCI//CASSCF-Energies of Transition States Levels Relative to That of 1a^a

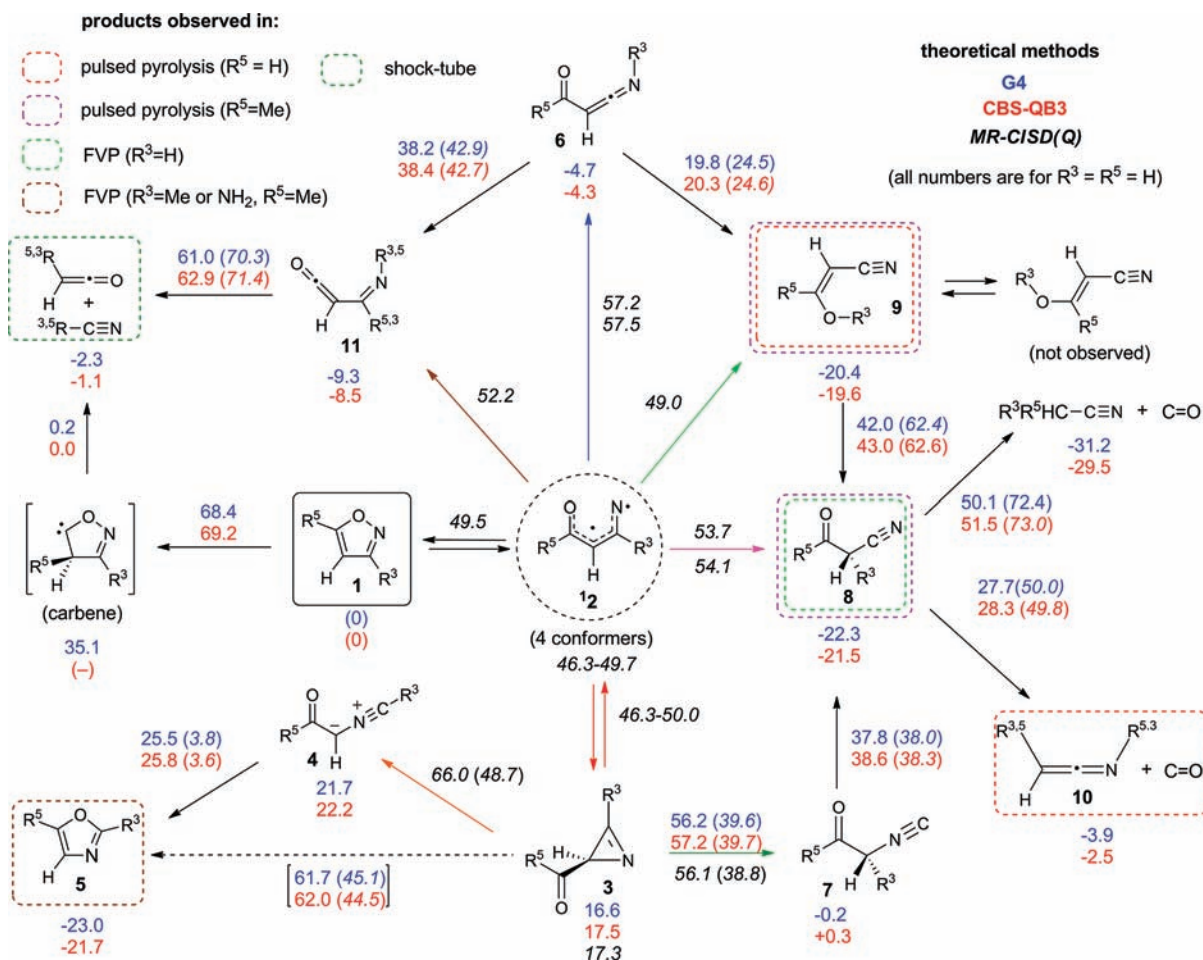
^a CS and OS stand for “closed shell” and “open shell”, respectively. For structures, see Figure S4 of the Supporting Information.

conformers) to the *syn*-(*Z*) conformer of the hydroxypropenenitrile **9a**, which was very gratifying to note because **9a** is the first product that is seen on pulsed pyrolysis of **1a** at the lowest temperature where decomposition is observed. Interestingly, the transition state for that reaction, which at the MRCI(Q) level lies slightly *below* that for the breaking of the N–O bond in **1a**, turned out to be almost planar, and its wave function is solidly closed shell, that is, the surface crossing must have occurred prior to the transition state, in the region leading up to it.

The next decay channel that becomes accessible at the MRCI(Q)/CASSCF level is that leading from *anti*-(*Z*)-**2a** to iminoketene **11a**, but since this product was not observed in the pulsed pyrolysis experiments, there must be another decay channel associated with lower barriers leading to the other observed products, that is, ketenimine + CO. The barriers for the [1,2]-H-

shifts from any of the conformers of **2a** to *syn*- or *anti*-formyl-nitrile **8a** are slightly higher than that for the decay to **11a** (they are also closed-shell in nature, and possibly they directly connect azirines **3a** to **8a**). The [1,2]-H-shifts leading from **2a** or **3a** to the (also unobserved) ketenimines **6a** have even higher barriers, so they will not be considered further.

The results of the above-described calculations are summed up in Scheme 7, which shows the energies of the transition states corresponding to the different decay channels relative to the energy of isoxazole **1a** (exact numbers and all structures are given in Table S5 and Figures S4 and S5 of the Supporting Information). We note that the relative energies of transition states that are of closed- and open-shell nature, respectively, are affected to surprisingly different extents by the Davidson correction for quadruple excitations (“Q”) to the MR-CISD results. The origin

Scheme 8. Pathways for Secondary Rearrangements and Cleavages of Primary Products of the Pyrolysis of Isoxazoles^a

^a All numbers are energies in kcal/mol for the parent compounds, that is, $R^3 = R^5 = H$, relative to isoxazole, **1a**. The numbers next to the arrows are energies of transition states (those in parentheses are relative to the preceding minimum). The colors of the arrows are consistent with those in Scheme 6. Note that a direct pathway leading from **3** to **5** probably does not exist (discussion, see text). Structures are depicted in Figures S4 and S5 of the Supporting Information.

of this discrepancy will be analyzed in a separate paper, but we will base our discussion on the MR-CISD(Q) results (actually, it turns out that the chemical conclusions are not affected by this choice).

2.3.3. Rearrangements of the Primary and Formation of Secondary Products. Some of the products observed in one or the other type of thermolysis experiment are formed by pathways that do not involve the carbonylvinylidene nitrenes, and in this section, we will discuss these. Because multideterminant methods are not needed to calculate the structures and transition states here, we will base our discussion on results from two high-level composite procedures, the CBS-QB3 method of Petersson et al.⁴⁸ and the G4 method of Curtiss et al.⁴⁹ (for details, see Methods). Scheme 8 sums up the corresponding energies including ZPV contributions relative to isoxazole or, for transition states, also relative to the reactants, respectively (in parentheses).

The first question that we will address concerns the formation of ketenimine **10** + CO, which was observed in the pulsed pyrolysis of parent isoxazole **1a** (but *not* of its 5-methyl derivative, **1b**). These products must arise by cleavage of a compound that has a carbonyl group and a C–C–N moiety of which only two may be formed directly from isoxazole, namely, ketenimine **6** and

ketenitrile **8**. In both cases, a migration of R^5 is required to occur in concert with the C–C cleavage ([1,2] in the case of **6**, [1,4] in the case of **8**), which explains why this cleavage is suppressed when $R^5 = CH_3$ (see Scheme S3 in the Supporting Information). Because instead **8** is observed on pyrolysis of **1b**, we focused on the cleavage of **8** in the case where $R^5 = H$. Indeed we found a rather low-lying transition state involving H-migration from the carbonyl group to the N-atom and concurrent C–C cleavage. If the temperature is high enough to induce rearrangement of **1a** to form **8**, then there is also enough energy available for the cleavage of the latter compound to **10** + CO, even if partial thermalization takes place in the molecular beam.

If **10** is formed from nitrile **8**, then the question arises whether **8** could be formed by a lower energy pathway than that which involves the vinylidene nitrenes **2**. There are two possibilities: (a) by ketonization of the Z-hydroxypropenenitrile **9** or (b) by rearrangement of azirine **3** to the isonitrile **7** (by way of C–C cleavage + migration of R^3), which may then isomerize to nitrile **8**. Which pathway is followed will depend on how rapidly the primary products, **3** and **9**, can dissipate their excess energy under the conditions of an experiment: If thermalization is complete, then the complicated rearrangement of azirine **3** to isonitrile **7** involves

indeed a much lower barrier (ca. 39 kcal/mol) than ketonization of **9** (ca. 62 kcal/mol). Conversely, if there is no thermalization then the ketonization of **9** is spontaneous (because the barrier for this process is lower than that for the formation of **9**), whereas the rearrangement of **3** to **7** involves a barrier that is on the same order as that for direct formation of **8** from **2**.

Thus the most advantageous pathway for the formation of **8** depends on the experimental conditions. The fact that if $R^5 = \text{CH}_3$, that is, if cleavage of **8b** is prohibited, hydroxypropenenitrile **9b** persists under the conditions of pulsed pyrolysis seems to indicate that nitrile **8b** may be formed (also) in other ways than by ketonization of **9b**. However, additional experiments would be needed to settle this question. If $R^3 \neq \text{H}$, then **8** should not be formed at all because it invariably involves a shift of R^3 . Indeed it was found that, if $R^3 \neq \text{H}$ then carbonylnitriles **8** were not observed in flash vacuum pyrolysis of isoxazole derivatives.¹⁴

A third question involves the mechanism of formation of oxazole **5**, which is the only observed product if both R^3 and R^5 are not H-atoms. In this case, all rearrangements that involve migrations of either of these substituents (i.e., formation of **6–11**) are suppressed, so that decay to azirines **3** is the only viable (nondissociative) deactivation pathway. Indeed, this product was observed on flash vacuum pyrolysis of 3,4-dimethyl-5-aminoisoxazole at moderate temperature, whereas on pyrolysis of 3,5-dimethyl- and 3-amino-5-methylisoxazole at higher temperatures, 2,5-disubstituted oxazoles were the only observed products.¹⁴ This indicates that a pathway is available for rearrangement of carbonylazirines **3** to oxazoles **5**.

It has been demonstrated that in photochemical reactions of (aryl)2*H*-azirines, this rearrangement proceeds via a nitrile ylide **4**,²⁷ and it has been postulated that **4** is also involved in the thermal process.^{10,50} Our calculations show that one can indeed find a transition state for this C–C ring-opening reaction, but the RHF wave function at this transition state turns out to be unstable. Thus we located the same transition state by the CASSCF method, and we found indeed that the wave function has significant open shell character, so the calculation of the activation barrier for this process requires a multiconfigurational wave function. Hence we characterized the C–C ring-opening pathway of azirine **3a** by CASSCF with an active space that is consistent for that process (but which is not identical to that used for the reactions leading to or from the vinylnitrenes, see Methods section). At the MRCISD(Q) level, the barrier for this reaction is almost 50 kcal/mol if one starts from thermalized azirine **3a** and over 67 kcal/mol relative to isoxazole **1a**. The ring closure of singlet nitrile ylide **4a** to oxazole **5a** (both of which are solidly closed-shell compounds) is very exothermic and has a very low barrier.⁵¹ At the DFT level, one can also find a transition state (with a stable wave function) for the **3a** → **5a** rearrangement, which bypasses the nitrile ylide, but all attempts to locate this transition state at the CASSCF level failed or led to the open-shell transition state leading to **4**. Thus we conclude that this lowering “concerted” transition state is an artifact of constraining the system to remain on the closed-shell surface throughout this reaction.

As a conclusion of the above, our calculations have shown that, under conditions where the N–O bond in isoxazoles **1** can be cleaved, azirines **3** form spontaneously and equilibrate (enantiomerize) via vinylnitrenes **2**. As the temperature is raised, H-shifts begin to kick in and eventually siphon off the vinylnitrenes. If R^3 or R^5 are methyl groups some or all of these channels are blocked

and ring-opening of the azirines to yield nitrile ylides **4** and eventually oxazoles **5** takes over.

Finally, we can try to account, on the basis of our calculations, for the decomposition products that were observed in the shock-tube experiments,¹⁶ where apparently much more energy was available to drive cleavage reactions. In the case of **1a**, the major products were ketene + HCN, which were hypothesized to arise by decomposition of the carbene that is formed from **1a** by a [1,2]-H shift. This shift involves, however, a fairly high barrier (ca. 69 kcal/mol), but on the other hand, the carbene that is formed decomposes in a practically activationless process. Alternatively, $\text{H}_2\text{C}=\text{CO} + \text{HCN}$ may be formed by way of iminoketene **11a**, which undergoes a [1,3] (N–C)-H-shift, concomitant with cleavage of the C–C bond. Although, if one starts from thermalized precursors, the barrier for this process is higher than that for the formation of the carbene, the second process becomes competitive if thermalization is incomplete.

The formation of $\text{CH}_3\text{CN} + \text{CO}$ may occur by [1,2]-H-shift plus C–C bond cleavage from carbonylnitrile **8**. Again the barrier for this process is high, but if excess energy from the formation of **8** is available to drive the process, it may be competitive with some of the rearrangements in Scheme 8 (an alternative path, starting from ketenimine **6** and involving two successive H-shifts, was found to have a much higher activation energy). Other products that were observed in the shock-tube studies, such as CO_2 , methane, and ethane, cannot be accounted for in terms of unimolecular processes.

We also calculated the barriers for the processes leading to the observed products for the case where $R^5 = \text{Me}$, that is, the pyrolysis of **1b**. All the transition states were located on the CAS(8,7)SCF surface, but it turned out that the barriers for cleavage of the N–O bond in **1b** as well as those leading to ketonitrile **8b** and its enol form, hydroxybutenenitrile **9b**, were within a kcal/mol of those in the parent compounds (see Supporting Information). When the position 3 is also occupied by a methyl group (3,5-dimethylisoxazole, **1c**), all the reaction channels that involve migration of R^3 and R^5 are blocked, which leaves only azirine **3c** and oxazole **5c** as possible rearrangement products. However, new (dissociative) reaction channels appear to open up, which will, however, not be discussed in the present paper.

3. METHODS

3.1. Pulsed Pyrolysis. In order to study the pyrolysis of isoxazoles **1a**, **1b**, and **1c**, we used a pulsed pyrolyzer system, based on the design conceived by Chen and co-workers,⁵² developed in the Integrated Instrument Development Facility (IIDF) of the Cooperative Institute for Research on Environmental Sciences (CIRES) of the University of Colorado in Boulder.⁵³

In this instrument, 5 ms pulses of a host gas (in our case Ar at ca. 800 mbar) seeded with ca. 0.1% of the precursor to be pyrolyzed are passed through a resistively heated 25 mm × 1 mm ID silicon carbide (SiC) tube, the temperature of which can be maintained at ±5 °C up to ca. 1200 °C. In contrast to flash vacuum pyrolysis (FVP) where the activation occurs primarily by contact with the wall of the pyrolysis tube (or of added material therein), the activation in this experiment occurs almost exclusively by collision with the hot host gas atoms, which are entirely unreactive, which largely avoids unwanted side reactions.

The pyrolyzer was flanged onto a cryostat based on an APD Cryogenics closed-cycle helium refrigeration system with DE-202A expander. Thus, the output of the SiC tube is directed to the CsI window that is used as optical substrate for the matrices. During

deposition of the pyrolysis products, the temperature of the CsI window was stabilized between 15 and 20 K.

Isoxazole **1a** (99% purity) and 3,5-dimethylisoxazole **1c** (98% purity) were purchased from Aldrich. 5-Methylisoxazole **1b** (>95% purity) was purchased from TCI Europe. Authentic samples of 2-acetyl-3-methyl-2H-azirine **3c** and 2,5-dimethylloxazole **5c** were prepared according to a literature procedure.^{8,54} 2-Acetyl-3-methyl-2H-azirine **3c**, $UV_{\max} = 254$ nm (ACN). ¹H NMR (400 MHz, CDCl₃): $\delta_c = 2.05$ (3H, s); 2.54 (3H, s); 2.84 (1H, s). ¹³C NMR (125 MHz, CDCl₃): $\delta_c = 13.1$, 27.3, 36.9, 159.5, 207.2. 2,5-Dimethylloxazole **5c**, $UV_{\max} = 208$ nm (ACN). ¹H NMR (400 MHz, CDCl₃): $\delta = 2.26$ (3H, s); 2.39 (3H, s); 6.59 (1H, s).

Prior to usage, the samples were degassed by using the standard freeze–pump–thaw method, whereupon the precursor vapor was premixed with high-purity argon in ratios ranging from 1:500 to 1:2000 in a 3 L Pyrex glass reservoir to a pressure of 800 mbar, using standard manometric techniques. During the experiments, the flux of the mixture was controlled by reading the drop pressure in the reservoir with a capacitance manometer. In a typical experiment, the pulsed valve operated with an opening time of 5 ms and pulse frequency of 12 Hz during 1000 to 3000 s.

Photochemical transformations of the matrix-isolated pyrolysis products were induced using the frequency-doubled signal beam provided by a Quanta-Ray MOPO-SL optical parametric oscillator (fwhm ≈ 0.2 cm⁻¹) pumped with a pulsed Nd:YAG laser (repetition rate = 10 Hz, pulse energy ≈ 5 mJ, duration = 10 ns).

The IR spectra, in the 4000–400 cm⁻¹ range, were obtained using a Mattson (Infinity 60AR series) Fourier transform infrared spectrometer, equipped with a deuterated triglycine sulfate (DTGS) detector and a Ge/KBr beam splitter with 0.5 cm⁻¹ spectral resolution. To avoid interference from atmospheric H₂O and CO₂, a stream of dry air was continuously purged through the optical path of the spectrometer.

3.2. Quantum Chemical Calculations. For the purpose of modeling IR spectra, the geometry optimization and the frequency calculations were done with the B3LYP/6-311+G(d,p) method. After scaling the calculated frequencies by factors of 0.980 below 3000 cm⁻¹ and 0.950 above 3000 cm⁻¹, the resulting frequencies, together with the calculated intensities, served to simulate the spectra shown in the figures by convoluting each peak with a Lorentzian function with a full width at half-maximum (fwhm) of 2 cm⁻¹, so that the integral band intensities correspond to the calculated infrared absolute intensity.⁵⁵ Note that the peak intensities in the simulated spectra are several times less (in the arbitrary units of “relative intensity”) than the calculated intensity (in km mol⁻¹).

In the regions of the potential surface where open-shell singlet states do not intervene during the reactions that interconvert different species (see below), we resorted to the CBS-QB3⁴⁸ and the G4 methods⁴⁹ to get reliable relative energies. Both of these methods imply geometry optimizations and frequency calculations by the B3LYP density functional method (with differently polarized 6-31G(d,p)-type basis sets for the two methods), followed by series of single-point calculations that are designed to capture the effects of going to very large basis sets, either by direct extrapolation (CBS-QB3) or in an additive fashion (G4). Eventually, both methods aim at estimating the result of a CCSD(T) calculation with a very large basis set, supplemented by empirical corrections to account for relativistic or spin–orbit coupling effects. Generally, both methods are thought to be accurate to within 1 kcal/mol. It is gratifying to note that the results obtained by both methods rarely diverge by more than that amount.

All calculations described above were carried out with the Gaussian program package.⁵⁶

For the processes that involve the formation or decay of open-shell carbonylvinylnitrenes, we used the multiconfigurational complete active space self-consistent field (CASSCF) method with the 6-31G* basis set

to find stationary points (we checked that the geometries do not change significantly on enlarging the basis set, see Figure S11 and Table S9 in the Supporting Information). At these geometries, we carried out single-point calculations at the multireference configuration interaction (MRCI) level including all single and double excitations (SD) with the cc-pVTZ basis set (we ascertained that at this level the results are close to converged with regard to the basis set limit, see Figure S12 in the Supporting Information). In studies of chemical reactions by these methods, it is very important to choose an active space that contains all the MOs and the electrons that change along the considered pathways, to avoid discontinuities of the potential surfaces and to be able to compare energies. Eventually we found that an active space containing eight electrons in seven active orbitals allowed us to fulfill this condition, provided that it contained the right orbitals (see below). Since the reactions involve passages between open- and closed-shell singlet states, we used state-averaged orbitals throughout all calculations.

In the case of isoxazole, those were the five π/π^* -MOs containing the six π -electrons and the N–O σ - and σ^* -MOs. In the vinylnitrenes, the N–O orbitals were replaced by the singly occupied in-plane p-AO of N and the in-plane p-lone pair of O, while in the azirine **3** one of the π/π^* pairs turns into the σ - and σ^* -MOs of the newly formed C–N bond. It was not possible to find a compatible active space for the other primary products (**6**, **8**, **9**, and **11**), but we profited from the fact that the transition states for formation of these products are very early (because the reactions are exothermic by over 55–70 kcal/mol), so the active space that we used for the vinylnitrenes **2** was used to describe also those transition states because we had to use a consistent active space to ensure comparability of energies. This active space does not explicitly contain the σ - and σ^* -MOs of the reactive X–H bonds because we were not able to include those MOs in the vinylnitrenes. All these MOs are depicted in Figures S6–S8 of the Supporting Information.

It turned out that the active space needed to describe the transition states leading from **3a** to both **4a** and **7a** is not consistent with that described above. Instead of the σ - and σ^* -MOs of the C–N bond in **3a**, those of the C–C bond in the azirine ring were included. In order to make all MRCI relative energies comparable, we recomputed also the geometries and the energies of azirine **3a** with this active space. These orbitals are depicted in Figure S9 and S10 of the Supporting Information).

All transition states (TS) were characterized by intrinsic reaction coordinate (IRC) calculations, which led to the starting vinylnitrenes on one side and to the closed-shell products on the other side, sometimes after optimization at the end of an IRC path. The three TS leading from the vinylnitrenes **2a** to the azirines **3a** (and the *anti*-(*Z*)-vinylnitrene, which is itself already a transition state for the interconversion of enantiomeric azirines) were of predominant open-shell nature, that is, they occur before the crossing to the closed-shell singlet surface of the azirine. The wave function of the TS for the N–O cleavage of isoxazole **1a** was found to consist of similar parts of closed- and open-shell configurations, that is, that TS lies very close to the conical intersection of the two crossing surfaces (cf. Scheme 5).

The wave functions for the TSs for the very exothermic decay of the vinylnitrenes **2a** to the stable products **6**, **8**, **9**, and **11** were all predominantly closed-shell, so they lie *after* the crossings of the open- and closed-shell singlet surfaces, which therefore appear to occur quite close to the vinylnitrenes, despite the fact that the first (predominantly closed shell) excited state of these vinylnitrenes lies ca. 10–12 kcal/mol above the lowest open-shell state. This can be explained by the fact that the open-shell singlet surface, which leads to excited states of the products (cf. Scheme 6) is, at least initially, quite flat, whereas the closed-shell surface that cuts through it and leads to the product ground states is very steep, because these reactions are very exothermic. The details of this will be discussed in a forthcoming paper.

All CASSCF and MRCI calculations were done with the Molpro program package.⁵⁷ All energies are listed in Tables S5–S8 of the

Supporting Information, which contains also the Cartesian coordinates of all stationary points.

4. CONCLUSIONS

We have studied the pyrolysis of parent isoxazole, **1a**, and of its 5-methyl and 3,5-dimethyl derivatives, **1b** and **1c**, respectively, by the high-pressure pulsed pyrolysis method, where activation of the precursor molecules occurs by collisions with the host gas (Ar in our case), rather than with the walls of the pyrolysis tube, where catalyzed processes may occur. The products were trapped at 15 K in Ar matrices where they were characterized by vibrational spectroscopy. Thereby we found a hitherto unobserved primary product of pyrolysis of isoxazole, the 3-hydroxypropenenitrile **9a**, or its methyl derivative **9b**. *E-Z* photoisomerization could be induced in compounds **9**.

On pyrolysis of **1a**, ketenimine **10** and CO were observed as decomposition products, but this process did not occur when the 5-methyl derivative, **1b**, was pyrolyzed. Instead, ketonitrile **8b** was formed. In the case of 3,5-dimethylisoxazole **1c**, acetylazirine **3c** was detected at lower temperatures, whereas at higher temperatures, 2,5-dimethyloxazole **5c** was the only observed rearrangement product (next to products of dissociation, which will be discussed separately).

We have rationalized the above findings on the basis of quantum chemical calculation. Thereby it became evident that carbonyl-vinylnitrenes **2** play a pivotal role in the observed rearrangements, a role that had not been recognized in previous theoretical studies because it had been assumed that vinylnitrenes are closed-shell singlet species, whereas they are in fact open-shell singlet biradicaloids. Thus, the primary processes had to be modeled by the multiconfigurational CASSCF method, followed by single-point MR-CISD calculations. The picture that emerges from these calculations is in excellent accord with the experimental findings, that is, they explain why some possible products are observed while others are not.

■ ASSOCIATED CONTENT

S Supporting Information. Tables listing the observed IR peaks and their assignment based on B3LYP calculations, full IR spectra for the pyrolysis of **1b** and **1c**, energies and structures of the stationary points found on the CASSCF and B3LYP (G4) potential surfaces, orbitals contained in the active space for compounds subjected to MRCISD//CASSCF calculations, basis-set dependence of the MRCISD results, Cartesian coordinates of all stationary points discussed in this study, full references for the Gaussian⁵⁶ and Molpro⁵⁷ program packages. This material is available free of charge via the Internet at <http://pubs.acs.org>.

■ AUTHOR INFORMATION

Corresponding Author

reva@qui.uc.pt; thomas.bally@unifr.ch

Note

[†]On leave from Masaryk University, Brno, Czech Republic.

■ ACKNOWLEDGMENT

These studies were partially funded by the Portuguese "Fundação para a Ciência e a Tecnologia" (FCT) Projects PTDC/QUI/71203/2006-No. FCOMP-01-0124-FEDER-007458, PTDC/

QUI-QUI/111879/2009, and PTDC/QUI-QUI/118078/2010, cofunded by QREN-COMPETE-UE. C. M. Nunes acknowledges FCT for Grant No. SFRH/BD/28844/2006. The work is also part of project No 200020-132005 of the Swiss National Science Foundation. T.S. profited from a stipend of the SCIEIX (Scientific Exchange Programme between Switzerland and the New Member States of the EU) program of the Swiss Confederation and of the Brno Ph.D. Talent program sponsored by Brno City Municipality. We are very indebted to Prof. Paul Rablen (Swarthmore College) who carried out many of the G4 calculations.

■ REFERENCES

- (1) *Comprehensive Heterocyclic Chemistry*; Lang, S. A., Lin Jr., Y.-I., Eds.; Pergamon: Oxford, 1984; Vol. 6, Part 4B.
- (2) *Chemistry of Heterocyclic Compounds*; Grünanger, P., Vita-Finzi, P., Eds.; John Wiley and Sons, 1991; Vol. 47, Part 1.
- (3) Dalvie, D. K.; Kalgutkar, A. S.; Khojasteh-Bakht, S. C.; Obach, R. S.; O'Donnell, J. P. *Chem. Res. Toxicol.* **2002**, *15*, 269.
- (4) Kalgutkar, A. S.; Nguyen, H. T.; Vaz, A. D. N.; Doan, A.; Dalvie, D. K. *Drug Metab. Dispos.* **2003**, *31*, 1240.
- (5) Yu, J.; Folmer, J. J.; Hoesch, V.; Doherty, J.; Campbell, J. B.; Burdette, D. *Drug Metab. Dispos.* **2011**, *39*, 302.
- (6) Pinho e Melo, T. M. V. D. *Curr. Org. Chem.* **2005**, *9*, 925.
- (7) Murature, D. A.; Perez, J. D.; Debortorello, M. M.; Bertorello, H. E. *Anal. Asoc. Quim. Argentina* **1976**, *64*, 337.
- (8) Perez, J. D.; de Diaz, R. G.; Yranzo, G. I. *J. Org. Chem.* **1981**, *46*, 3505.
- (9) Perez, J. D.; Yranzo, G. I.; Wunderlin, D. A. *J. Org. Chem.* **1982**, *47*, 982.
- (10) Perez, J. D. *Anal. Asoc. Quim. Argentina* **1983**, *71*, 99.
- (11) Perez, J. D.; Wunderlin, D. A. *Int. J. Chem. Kinet.* **1986**, *18*, 1333.
- (12) Perez, J. D.; Wunderlin, D. A. *J. Org. Chem.* **1987**, *52*, 3637.
- (13) Wunderlin, D. A.; Davico, G. E.; Perez, J. D. *Int. J. Chem. Kinet.* **1992**, *24*, 31.
- (14) Yranzo, G. I.; Moyano, E. L. *Curr. Org. Chem.* **2004**, *8*, 1071.
- (15) Davico, G. E. *J. Phys. Org. Chem.* **2005**, *18*, 434.
- (16) Lifshitz, A.; Wohlfeiler, D. *J. Phys. Chem.* **1992**, *96*, 4505.
- (17) Lifshitz, A.; Wohlfeiler, D. *J. Phys. Chem.* **1992**, *96*, 7367.
- (18) Okada, K.; Saito, K. *J. Phys. Chem.* **1996**, *100*, 9365.
- (19) Higgins, J.; Zhou, X. F.; Liu, R. F. *J. Phys. Chem. A* **1997**, *101*, 7231.
- (20) Parasuk, V.; Cramer, C. J. *Chem. Phys. Lett.* **1996**, *260*, 7.
- (21) Karney, W. L.; Borden, W. T. *J. Am. Chem. Soc.* **1997**, *119*, 1378.
- (22) Rajam, S.; Murthy, R. S.; Jadhav, A. V.; Li, Q.; Keller, C.; Carra, C.; Pace, T. C. S.; Bohne, C.; Ault, B. S.; Gudmundsdottir, A. D. *J. Org. Chem.* **2011**, DOI: 10.1021/jo200877k.
- (23) Palmer, M. H.; Larsen, R. W.; Hegelund, F. *Mol. Phys.* **2004**, *102*, 1569.
- (24) Hegelund, F.; Larsen, R. W.; Nicolaisen, F. M.; Palmer, M. H. *J. Mol. Spectrosc.* **2005**, *229*, 244.
- (25) Robertson, E. G. *J. Mol. Spectrosc.* **2005**, *231*, 50.
- (26) Abe, H.; Takeo, H.; Yamada, K. M. T. *Chem. Phys. Lett.* **1999**, *311*, 153.
- (27) Inui, H.; Murata, S. *J. Am. Chem. Soc.* **2005**, *127*, 2628 and references cited therein.
- (28) Finnerty, J.; Mitschke, U.; Wentrup, C. *J. Org. Chem.* **2002**, *67*, 1084.
- (29) Kurtz, D. W.; Shechter, H. *Chem. Commun.* **1966**, 689.
- (30) Cumulated double bond stretches often show pronounced site splitting in cryogenic matrices, which is why this band appears as a pair separated by 2 cm⁻¹ (2039 and 2037 cm⁻¹).
- (31) The product absorption band at 1632/1627 cm⁻¹ is at too low frequency to be attributed to the aldehyde $\nu(\text{C}=\text{O})$ mode of formylketenimine **6a**, which is predicted by the B3LYP/6-311++G(d,p) calculation as a strong band at 1711 and 1702 cm⁻¹ (originating from two possible conformations).

- (32) Guennoun, Z.; Couturier-Tamburelli, I.; Combes, S.; Aycard, J. P.; Pietri, N. *J. Phys. Chem. A* **2005**, *109*, 11733.
- (33) Jacox, M. E. *Chem. Phys.* **1979**, *43*, 157.
- (34) Jacox, M. E.; Milligan, D. E. *J. Am. Chem. Soc.* **1963**, *85*, 278.
- (35) Bernstein, M. P.; Sandford, S. A.; Allamandola, L. J. *Astrophys. J.* **1997**, *476*, 932.
- (36) Reisenauer, H. P.; Romanski, J.; Mloston, G.; Schreiner, P. R. *Eur. J. Org. Chem.* **2006**, 4813.
- (37) Schreiner, P. R.; Reisenauer, H. P. *Angew. Chem., Int. Ed.* **2008**, *47*, 7071.
- (38) Schreiner, P. R.; Reisenauer, H. P.; Pickard, F. C.; Simmonett, A. C.; Allen, W. D.; Matyus, E.; Csaszar, A. G. *Nature* **2008**, *453*, 906.
- (39) Schreiner, P. R.; Reisenauer, H. P.; Romanski, J.; Mloston, G. *Angew. Chem., Int. Ed.* **2009**, *48*, 8133.
- (40) Gerbig, D.; Reisenauer, H. P.; Wu, C. H.; Ley, D.; Allen, W. D.; Schreiner, P. R. *J. Am. Chem. Soc.* **2010**, *132*, 7273.
- (41) ΔG calculated at the CBS-QB3 level at temperatures between 300 and 700 °C; for details, see Supporting Information
- (42) Assuming a barrier of 65 kcal/mol for the rotation around the double bond in ethylene, and radical stabilization energies of 8.7 kcal/mol for an OH and 7.8 kcal/mol for a CN group acting at the perpendicular transition state, the barrier for rotation around the double bond in **9a** is estimated to be 48.5 kcal/mol, very close to the calculated barrier for cleavage of the N–O bond in **1a** (see section on mechanistic modeling): Menon, A. S.; Wood, G. P. F.; Moran, D.; Radom, L. *J. Phys. Chem. A* **2007**, *111*, 13638.
- (43) Felder, P.; Günthard, H. H. *Chem. Phys. Lett.* **1979**, *66*, 283.
- (44) Felder, P.; Günthard, H. H. *Chem. Phys.* **1982**, *71*, 9.
- (45) Kudoh, S.; Takayanagi, M.; Nakata, M. *Chem. Phys. Lett.* **1998**, *296*, 329.
- (46) Vidya, V.; Sankaran, K.; Viswanathan, K. S. *Chem. Phys. Lett.* **1996**, *258*, 113.
- (47) According to B3LYP calculations, the intensities of these bands (which, after scaling by 0.98, are predicted at 2068 cm^{-1} for **6b** and at 2172 cm^{-1} for **7b**) should be equal to or stronger than that of the C=O stretching vibration.
- (48) Montgomery, J. A.; Frisch, M. J.; Ochterski, J. W.; Petersson, G. A. *J. Chem. Phys.* **1999**, *110*, 2822.
- (49) Curtiss, L. A.; Redfern, P. C.; Raghavachari, K. *J. Chem. Phys.* **2007**, *126*, No. 084108.
- (50) Davico, G. E.; Perez, J. D. *J. Phys. Org. Chem.* **1990**, *3*, 611.
- (51) The barrier might be higher in aryl derivatives of ylide **4**, which have been intercepted by dienophiles and have been trapped and observed in Ar matrices.
- (52) Kohn, D. W.; Clauber, H.; Chen, P. *Rev. Sci. Instrum.* **1992**, *63*, 4003.
- (53) <http://cires.colorado.edu/iidf/machine/pyrolyzer.html> (accessed August 15, 2011).
- (54) Sato, T.; Yamamoto, K.; Fukui, K.; Saito, K.; Hayakawa, K.; Yoshiie, S. *J. Chem. Soc., Perkin Trans. 1* **1976**, 783.
- (55) Irikura, K. K. Program SYNSPEC. Natl. Inst. Standards and Technol., Gaithersburg, MD 20899, USA. <http://www.ccl.net/cca/software/MS-DOS/synthetic-spectrum/SYNSPEC.TXT.shtml> (accessed August 15, 2011).
- (56) Frisch, M. J. et al. *Gaussian 03 and Gaussian 09*; Gaussian, Inc.: Wallingford, CT, <http://www.gaussian.com> (full citation see page S34 of the Supporting Information).
- (57) Werner, H. J. et al. *MOLPRO, version 2010.1*, Cardiff, UK., <http://www.molpro.net> (full citation, see page S35 of the Supporting Information).